JOURNAL OF MODERN OPTICS, 2002,
VOL. 49, NO. 14/15, 2309–2323

Taylor & Francis
Taylor & Francis Group

Generation of pulsed polarization-entangled two-photon state via temporal and spectral engineering

YOON-HO KIM and WARREN P. GRICE

Center for Engineering Science Advanced Research, Computer Science and Mathematics Division, Oak Ridge National Laboratory, Oak Ridge, Tennessee 37831, USA; e-mail:kimy@ornl.gov

(*Received 15 February 2002; revision received 10 April 2002*)

Abstract. The quantum state of the photon pair generated from type-II spontaneous parametric downconversion pumped by an ultrafast laser pulse exhibits strong decoherence in its polarization entanglement, an effect which can be attributed to the clock effect of the pump pulse or, equivalently, to distinguishing spectral information in the two-photon state. Here, we propose novel temporal and spectral engineering techniques to eliminate these detrimental decoherence effects. The temporal engineering of the two-photon wavefunction results in a universal Bell-state synthesizer that is independent of the choice of pump source, crystal parameters, wavelengths of the interacting photons and the bandwidth of the spectral filter. In the spectral engineering technique, the distinguishing spectral features of the two-photon state are eliminated through modifications to the two-photon source. In addition, spectral engineering also provides a means for the generation of polarization-entangled states with novel spectral characteristics: the frequency-correlated state and the frequency-uncorrelated state.

1. Introduction

Quantum entanglement [1], once discussed only in the context of the foundations of quantum mechanics, is now at the heart of the rapidly developing field of quantum information science [2]. Many researchers are hoping to exploit the unique features of entangled states in order to surpass the 'classical limit' in applications such as quantum lithography [3], the quantum optical gyroscope [4], and quantum clock synchronization and positioning [5].

A particularly convenient and reliable source of entangled particles is the process of type-II spontaneous parametric downconversion (SPDC) [6–10], in which an incident pump photon is split into two orthogonally polarized lower-energy daughter photons inside a crystal with a $\chi^{(2)}$ nonlinearity. Initially, the photon pairs are entangled in energy, time and momentum, owing to the energy and momentum conservation conditions that govern the process. In addition, polarization entanglement may be obtained as a result of specific local operations on the photon pair [7–10]. An optical process such as this has the advantage that the photons, once generated, interact rather weakly with the environment, thus making it possible to maintain entanglement for relatively long periods of time.

In this paper, we propose and analyse efficient generation schemes for pulsed two-photon polarization-entangled states. Through temporal or spectral engin-

Journal of Modern Optics ISSN 0950–0340 print/ISSN 1362–3044 online
http://www.tandf.co.uk/journals
DOI: 10.1080/0950034021000011455

eering of the two-photon state produced in the type-II SPDC process pumped by a ultrafast laser pulse (ultrafast type-II SPDC), it is possible to generate pulsed polarization-entangled states that are free of any post-selection assumptions. Pulsed polarization-entangled states are an essential ingredient in many experiments in quantum optics. They are useful, for example, as building blocks for entangled states of three or more photons [11]. (In general, the SPDC process only results in two-photon entanglement.) Pulsed two-photon entangled states are also useful in practical quantum cryptography systems, since the well-known arrival times permit gated detection.

We begin in section 2 with a discussion of the limitations of the state-of-the-art techniques for the generation of polarization-entangled photon pairs. In section 3, we present a universal Bell-state synthesizer, which makes use of a novel interferometric method to temporally engineer the two-photon wavefunction. We follow up in section 4 with an analysis of the spectral properties of the two-photon wavefunction produced in ultrafast type-II SPDC. We then propose a method for the efficient generation of pulsed polarization entanglement via the spectral engineering of the two-photon wavefunction. We also discuss two two-photon polarization-entangled states with novel spectral characteristics: the frequency-correlated state and the frequency-uncorrelated state. Entangled states with such spectral properties might be useful for quantum-enhanced positioning and in multisource interference experiments.

2. Two-photon entanglement in ultrafast type-II spontaneous parametric downconversion

Let us briefly review one of the standard techniques for generating polarization entangled two-photon states via type-II SPDC [8–10]. A typical experimental set-up is shown in figure 1. A type-II nonlinear crystal is pumped with an ultraviolet (UV) laser beam and the orthogonally polarized signal and idler photons, which are in the near infrared, travel collinearly with the pump. After passing through a prism sequence to remove the pump, the signal–idler photon pair is passed through a quartz delay circuit (extraordinary–ordinary delay τ) before the beam splitter splits the SPDC beam into two spatial modes. A polarization analyser and a single-photon detector are placed at each output port of the beam splitter for polarization correlation measurements. In this case, the two quantum-mechanical amplitudes in which both photons end up at the same detector are not registered since only coincidence events are considered. That is, a state post-selection has been made [8, 9, 12]. A non-collinear type-II SPDC method developed later resolved this state post-selection problem and is usually regarded as the 'standard' method for generating polarization-entangled photon pairs [10].

Both the collinear and the non-collinear type-II SPDC methods work very well for the generation of polarization-entangled photon pairs when the UV pump laser is continuous wave (CW). In this case, however, there is no information available regarding the photons' arrival times at the detectors. Such timing information can be quite useful in certain applications, as discussed in section 1. If the UV pump has the form of an ultrafast optical pulse (about 100 fs), then the photon pair arrival times can be known within a time interval of the order of the pump pulse duration. However, it has been theoretically and experimentally shown that, in general,

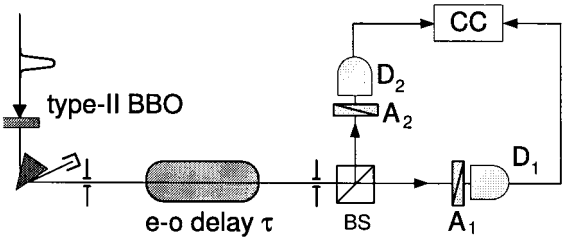

Figure 1. Typical experimental set-up for preparing a Bell state using collinear type-II SPDC: e–o, extraordinary–ordinary; BS beam splitter; BBO, β-barium borate; coincident counter (CC), D1, D_2, detectors; A_1, A_2 polarization analysers. Here, two out of four possible biphoton amplitudes are post-selected by the coincidence circuit, see [8, 9]. One can also utilize non-collinear type-II SPDC in which the amplitude post-selection assumption is not necessary [10].

type-II SPDC suffers the loss of quantum interference if the pump is delivered in the form of an ultrafast pulse [13, 14].

We shall first briefly review the theoretical treatment of the ultrafast type-II SPDC process and discuss the physical mechanism of the loss of quantum interference (or decoherence). With this understanding in hand, we then discuss in the subsequent sections two methods for eliminating this decoherence through spectral and temporal engineering of the two-photon state.

From first-order perturbation theory, the quantum state of type-II SPDC may be expressed as [9, 13]

$$|\psi\rangle = -\frac{\mathrm{i}}{\hbar}\int_{-\infty}^{\infty} \mathrm{d}t\, \mathcal{H}|0\rangle, \tag{1}$$

where

$$\mathcal{H} = \epsilon_0 \int \mathrm{d}^3\mathbf{r}\, \chi^{(2)} E_\mathrm{p}(z,t) E_\mathrm{o}^{(-)} E_\mathrm{e}^{(-)}$$

is the Hamiltonian governing the SPDC process. The pump electric field $E_\mathrm{p}(z,t)$ is considered classical and is assumed to have a Gaussian shape in the direction of propagation. The operator $E_\mathrm{o}^{(-)}$ ($E_\mathrm{e}^{(-)}$) is the negative frequency part of the quantized electric field of the ordinary polarized (extraordinary polarized) photon inside the crystal. Integrating over the length L of the crystal, equation (1) can be written as

$$|\psi\rangle = C\int\int \mathrm{d}\omega_\mathrm{e}\, \mathrm{d}\omega_\mathrm{o}\, \mathrm{sinc}\left(\frac{\Delta L}{2}\right) \mathcal{E}_\mathrm{p}(\omega_\mathrm{e}+\omega_\mathrm{o}) a_e^\dagger(\omega_\mathrm{e}) a_\mathrm{o}^\dagger(\omega_\mathrm{o})|0\rangle, \tag{2}$$

where C is a constant and $\Delta \equiv k_\mathrm{p}(\omega_\mathrm{p}) - k_\mathrm{o}(\omega_\mathrm{o}) - k_\mathrm{e}(\omega_\mathrm{e})$. The pump pulse is described by $\mathcal{E}_\mathrm{p}(\omega_\mathrm{e}+\omega_\mathrm{o}) = \exp[-(\omega_\mathrm{e}+\omega_\mathrm{o}-\Omega_\mathrm{p})^2/\sigma_\mathrm{p}^2]$, where σ_p and Ω_p are the bandwidth and the central frequency respectively of the pump pulse.

For the experimental set-up shown in figure 1, the electric field operators at the detectors are

$$E_1^{(+)} = \frac{1}{2^{1/2}} \int \mathrm{d}\omega' \, [\cos\theta_1 \, \mathrm{e}^{-\mathrm{i}\omega'(t_1+\tau)} a_\mathrm{e}(\omega') - \sin\theta_1 \, \mathrm{e}^{-i\omega' t_1} a_\mathrm{o}(\omega')],$$

$$E_2^{(+)} = \frac{\mathrm{i}}{2^{1/2}} \int \mathrm{d}\omega' \, [\cos\theta_2 \, \mathrm{e}^{-\mathrm{i}\omega'(t_2+\tau)} a_\mathrm{e}(\omega') + \sin\theta_2 \, \mathrm{e}^{-\mathrm{i}\omega' t_2} a_\mathrm{o}(\omega')],$$

where θ_1 and θ_2 are the angles of the polarization analysers A_1 and A_2, and τ is the extraordinary–ordinary delay. Here we have assumed no spectral filtering before detection. The coincidence count rate at the detectors is proportional to

$$\begin{aligned} R_\mathrm{c} &\propto \int \mathrm{d}t_1 \int \mathrm{d}t_2 \, |\langle 0|E_2^{(+)} E_1^{(+)}|\psi\rangle|^2 \\ &= \int \mathrm{d}t_+ \int \mathrm{d}t_- \, |\mathcal{A}(t_+, t_-)|^2, \end{aligned} \tag{3}$$

where $t_+ = (t_1 + t_2)/2$ and $t_- = t_1 - t_2$.

The two-photon amplitude $\mathcal{A}(t_+, t_-)$ has the form

$$\mathcal{A}(t_+, t_-) = \cos\theta_1 \sin\theta_2 \Pi(t_+, t_- + \tau) - \sin\theta_1 \cos\theta_2 \Pi(t_+, -t_- + \tau), \tag{4}$$

where

$$\Pi(t_+, t_-) = \begin{cases} \mathrm{e}^{-\mathrm{i}\Omega_\mathrm{p} t_+} \mathrm{e}^{-\sigma_\mathrm{p}^2 [t_+ - (D_+/D) t_-]^2} & \text{for } 0 < t_- < DL, \\ 0 & \text{otherwise.} \end{cases} \tag{5}$$

The parameters D_+ and D are defined to be

$$D_+ = \frac{1}{2}\left(\frac{1}{u_\mathrm{o}(\Omega_\mathrm{o})} + \frac{1}{u_\mathrm{e}(\Omega_\mathrm{e})}\right) - \frac{1}{u_\mathrm{p}(\Omega_\mathrm{p})},$$

$$D = \frac{1}{u_\mathrm{o}(\Omega_\mathrm{o})} - \frac{1}{u_\mathrm{e}(\Omega_\mathrm{e})},$$

where, for example, $u_\mathrm{o}(\Omega_\mathrm{o})$ is the group velocity of the orindary polarized photon of frequency Ω_o in the crystal.

It is clear from equations (3) and (4) that the degree of quantum interference is directly related to the amount of overlap between the two two-photon wavefunctions $\Pi(t_+, t_- + \tau)$ and $\Pi(t_+, -t_- + \tau)$. Figure 2 shows calculated two-photon

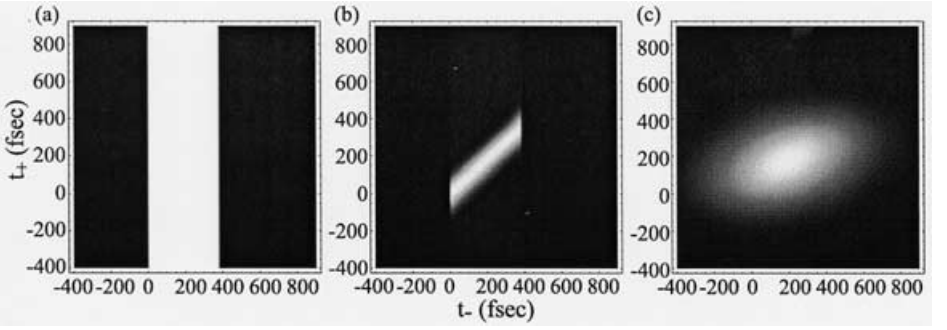

Figure 2. Calculated two-photon wavefunction $\Pi(t_+, t_-)$ for type-II SPDC. (*a*) For a CW-pumped case; the two-photon wavefunction is independent of t_+ and has a rectangular shape in t_-. (*b*) For a 100 fs pump pulse; it is strongly asymmetric. (*c*) With 5 nm bandwidth spectral filters; the two-photon wavefunction is expanded.

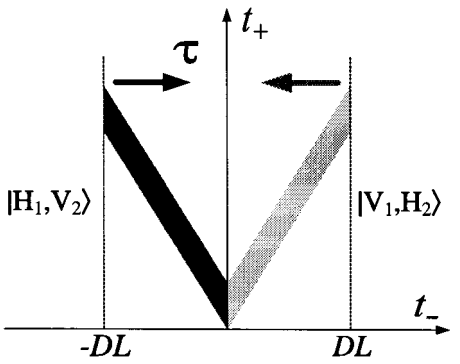

Figure 3. Distribution of two-photon amplitude $\mathcal{A}(t_+, t_-)$ for equation (4). Becuase of little overlap between $\Pi(t_+, t_- + \tau)$ and $\Pi(t_+, -t_- + \tau)$, quantum interference visibility cannot be high. In the CW-pumped case, however, 100% quantum interference should occur (see figure 2 (*a*)), if τ is correctly chosen.

wavefunctions for type-II SPDC in a 2 mm β-barium borate (BBO) crystal with a central pump wavelength of 400 nm. The two-photon wavefunction for the CW-pumped case is symmetric in t_+ and t_-. As shown in figure 2 (*a*), it has a rectangular shape in the t_- direction and extends to infinity in the t_+ direction. In the case of ultrafast type-II SPDC, the two-photon wavefunction is strongly asymmetric (see figure 2 (*b*)). As we shall show shortly, this is the origin of loss of quantum interference in ultrafast type-II SPDC.

Having learned the exact shape of the two-photon wavefunction $\Pi(t_+, t_-)$, we are now in a position to study the overlap of the wavefunctions in equation (4). The situation is well illustrated in figure 3. When $\tau = 0$, there is no overlap at all and hence no quantum interference. Increasing τ brings the two two-photon wavefunctions together and they begin to overlap. This increases the indistinguishability of the two wavefunctions, which represent the two-photon polarization states $|V_1, H_2\rangle$ and $|H_1, V_2\rangle$. Because the two wavefunctions are symmetric in CW-pumped type-II SPDC, perfect overlap may be achieved with the proper value of τ (see figure 2 (*a*)). With an ultrafast pump, however, the wavefunctions are asymmetric and perfect overlap is not possible. The amount of relative overlap may be increased in one of two ways: firstly, by decreasing the thickness of the crystal or, secondly, through the use of narrow-band spectral filters to expand the two-photon wavefunction (see figure 2 (*c*)). Both methods increase the relative amount of overlap, which in turn increase the overall indistinguishability of the system. The drawback of these methods, obviously, is the reduced number of available entangled photon pairs.

3. Temporal engineering of the two-photon state

In this section, we present a method in which complete overlap of two two-photon wavefunctions may be achieved with no change in the spectral properties of the photons. Consider the experimental set-up shown in figure 4. A type-II BBO crystal is pumped by either a CW-pumped or a pulse-pumped laser. As in [10] we restrict our attention to the photons found in the intersections of the cones made

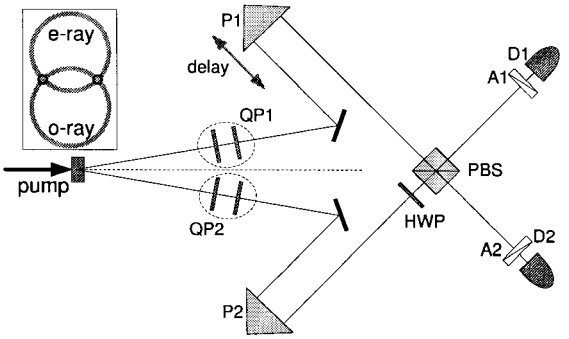

Figure 4. Universal Bell-state synthesizer: PBS, polarizing beam splitter; e-ray, extraordinary ray; o-ray, ordinary ray; D1, D2, detectors; A1, A2, polarization analysers; P1, P2, prisms. Non-collinear type-II SPDC is used to prepare an initial polarization state which is in a mixed state. QP1 and QP2 are thin quartz plates with optic axes oriented vertically and HWP is the $\lambda/2$ plate oriented at 45°.

by the extraordinary and ordinary rays exiting the crystal.† A $\lambda/2$ plate rotates the polarization in one arm before the two photons are brought together at a polarizing beam splitter. Note that since the two photons always have the same polarizations when they reach the polarizing beam splitter, they always exit different ports. Thus, the state post-selection assumption is not necessary.

The two Feynman alternatives (reflected–reflected and transmitted–transmitted) leading to coincidence detection are shown in figure 5. Note that there are only two two-photon amplitudes and in both cases the extraordinary ray (orindary ray) of the crystal is always detected by D_1 (D_2). This means that, unlike the experiment discussed in the previous section, any spectral or temporal differences between the orindary and extraordinary photons provide no information at the detectors that might make it possible to distinguish between the two wavefunctions. The two biphoton wavefunctions, which represent $|H_1\rangle|H_2\rangle$ and $|V_1\rangle|V_2\rangle$, are therefore quantum mechanically indistinguishable so that the state exiting the polarizing beam splitter is

$$|\Phi\rangle = \frac{1}{2^{1/2}}\left(|H_1\rangle|H_2\rangle + \mathrm{e}^{\mathrm{i}\varphi}|V_1\rangle|V_2\rangle\right),$$

where φ is the phase between the two terms. This phase may be adjusted by tilting the quartz plates QP1 and QP2. By setting $\varphi = 0$, the Bell state

$$|\Phi^{(+)}\rangle = \frac{1}{2^{1/2}}\left(|H_1\rangle|H_2\rangle + |V_1\rangle|V_2\rangle\right)$$

is attained. From this state, only simple linear operations are needed to transform to any of the other Bell states.

† The common misconception is that the photon pairs emerging from these two cross-sections are automatically polarization entangled. As we have discussed in section 2, the polarization state of the photon pair is in a mixed state:

$$\rho_{\mathrm{mix}} = \tfrac{1}{2}(|H_1\rangle|V_2\rangle\langle V_2|\langle H_1| + |V_1\rangle|H_2\rangle\langle H_2|\langle V_1|).$$

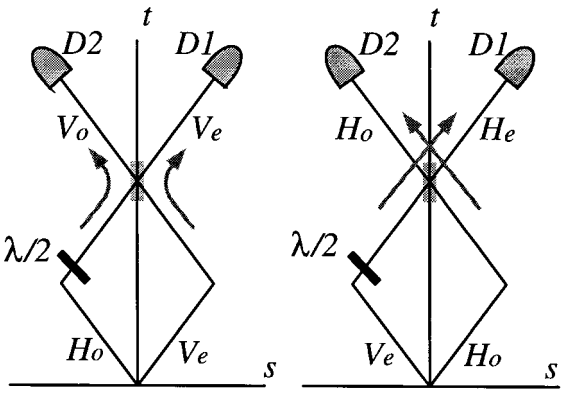

Figure 5. Feynman alternatives for the experimental set-up shown in figure 4. Note that the extraordinary-ray (ordinary-ray) of the crystal is always detected by D_1 (D_2) and there are only two two-photon alternatives (reflected–reflected and transmitted–transmitted). If the path length difference between the two arms of the interferometer is zero, the two alternatives (reflected–reflected and transmitted–transmitted) are indistinguishable in time regardless of the choice of the pump source, crystal thickness and spectral filtering.

Let us now analyse this interferometer more formally. If we assume that the phase difference between the two amplitudes φ is set to zero, then the electric field operators that reach the detectors may be written as

$$E_1^{(+)} = \int \mathrm{d}\omega' \, [\cos\theta_1 \, \mathrm{e}^{-\mathrm{i}\omega'(t_1+\tau)} a_{V\mathrm{e}}(\omega') - \sin\theta_1 \, \mathrm{e}^{-\mathrm{i}\omega' t_1} a_{H\mathrm{e}}(\omega')],$$

$$E_2^{(+)} = \int \mathrm{d}\omega' \, [\cos\theta_2 \, \mathrm{e}^{-\mathrm{i}\omega' t_2} a_{V\mathrm{o}}(\omega') - \sin\theta_2 \, \mathrm{e}^{-\mathrm{i}\omega'(t_2+\tau)} a_{H\mathrm{o}}(\omega')],$$

where, for example, $a_{V\mathrm{o}}(\omega')$ is the annihilation operator for a photon of frequency ω' with vertical polarization which was originally created as the ordinary ray of the crystal.

Then the two-photon amplitude $\mathcal{A}(t_+, t_-)$ may be expressed as

$$\mathcal{A}(t_+, t_-) = \cos\theta_1 \cos\theta_2 \Pi\left(t_+ + \frac{\tau}{2}, t_- + \tau\right)\Big) + \sin\theta_1 \sin\theta_2 \Pi\left(t_+ + \frac{\tau}{2}, t_- - \tau\right). \quad (6)$$

In contrast with the amplitude represented by equation (4), the two-photon wavefunctions on the right-hand side of equation (6) overlap completely when $\tau = 0$, regardless of their shape (figure 6). Since complete overlap is possible for any shape of the two-photon wavefunction, this method should work for both CW-pumped and pulse-pumped SPDCs. As such, this interferometer may be considered as a universal Bell-state synthesizer; perfect quantum interference may be observed regardless of pump bandwidth, crystal thickness or SPDC wavelength, with no need for spectral filters.

The typical peak-dip effect may be observed by varying the delay τ, that is

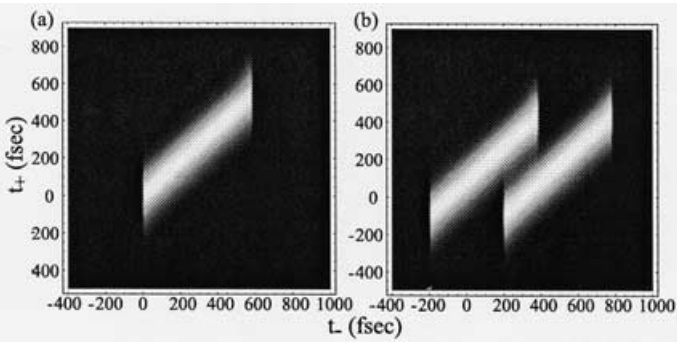

Figure 6. Temporally engineered two-photon amplitude. This figure shows how the two two-photon wavefunctions behave as τ is introduced. (*a*) Two two-photon wavefunctions overlap completely when $\tau = 0$ (compare with figure 3). (*b*) When $\tau = 200$ fs, there is almost no overlap.

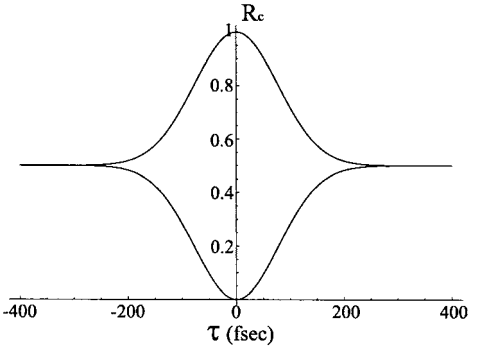

Figure 7. Calculated space–time interference pattern as a function of delay τ. The upper curve is for $\theta_1 = \theta_2 = 45^\circ$ and the lower curve is for $\theta_1 = -\theta_2 = 45^\circ$. The calculation is made for a 3 mm thick type-II BBO crystal pumped by a 400 nm pump pulse with bandwidth of approximately 2 nm.

$$R_c = \begin{cases} \dfrac{1}{2} + \dfrac{1}{2}\exp\left(\dfrac{-D_+^2\sigma_p^2\tau^2}{2D^2}\right) & \text{for } \theta_1 = \theta_2 = 45^\circ, \\ \dfrac{1}{2} - \dfrac{1}{2}\exp\left(\dfrac{-D_+^2\sigma_p^2\tau^2}{2D^2}\right) & \text{for } \theta_1 = -\theta_2 = 45^\circ. \end{cases}$$

Note that the thickness L of the crystal does not appear in the above equation and all other experimental parameters D_+, σ_p, and D only affect the width of the quantum interference, and not the maximum visibility. Figure 7 shows the calculated coincidence rate as a function of the delay τ. It is easy to see that the coincidence rate R_c is a slowly varying function of τ, with complete quantum interference expected at $\tau = 0$. This insensitivity to small changes in path length difference provides for a stable source of high-quality Bell states. This robustness is not found in two-crystal or double-pulse pump type-II SPDC schemes, where a small phase change in the interferometer results in sinusoidal modulations at

the pump central wavelength. Such schemes require active phase stabilization and, therefore, are not practical [15]. Our scheme does not suffer this disadvantage.

In addition, if $\tau \neq 0$, the amplitudes do not overlap completely and a more general state is generated:

$$\rho = \varepsilon\rho_{\text{ent}} + (1-\varepsilon)\rho_{\text{mix}},$$

where $\rho_{\text{ent}} = |\Phi^{(+)}\rangle\langle\Phi^{(+)}|$ and $0 \leqslant \varepsilon \leqslant 1$. Such partially entangled states are called Werner states and have recently been the subject of experimental studies in the CW domain [16]. Our scheme provides an efficient way to access a broad range of two-qubit states in both the pulsed and the CW domains.

4. Spectral engineering of the two-photon state

Using the temporal engineering technique discussed in the preceding section, it is possible to generate polarization entangled states with either CW-pumped or pulse-pumped schemes. It should be pointed out that neither the asymmetry of the two-photon wavefunction nor the spectral properties of the photon pairs are affected by this technique. In this section, we are interested in removing the asymmetry shown in figure 2 (*b*) through a careful choice of wavelengths of photons involved in the interaction. In this way, it is possible to obtain pulsed polarization-entangled photon pairs directly.

Recall that the source of poor wavefunction overlap in ultrafast type-II SPDC is the asymmetry introduced by a coupling between t_+ and t_- in the two-photon wavefunction given in equation (5). The approach here is to remove the coupling term so that the two-photon wavefunction becomes symmetric, as originally proposed by Keller and Rubin [13]. An example of such a wavefunction is shown in figure 8. Note that it has a rectangular shape in t_- (just as in CW-pumped type-II SPDC) and has a Gaussian shape in t_+ due to the Gaussian pulse envelope. It is not difficult to see that two-photon wavefunctions of this type may be completely overlapped, thus yielding full quantum interference. Therefore,

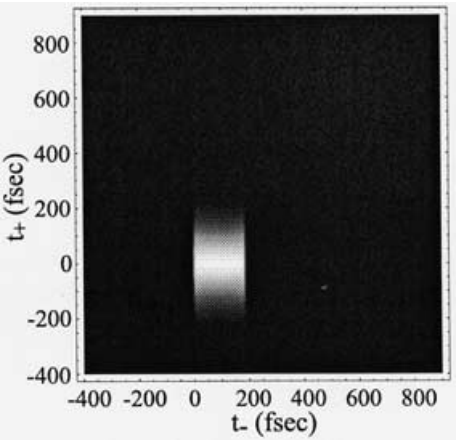

Figure 8. Spectrally engineered two-photon wavefunction. Note that the asymmetry shown in figure 2 (*b*) has disappeared. See text for details.

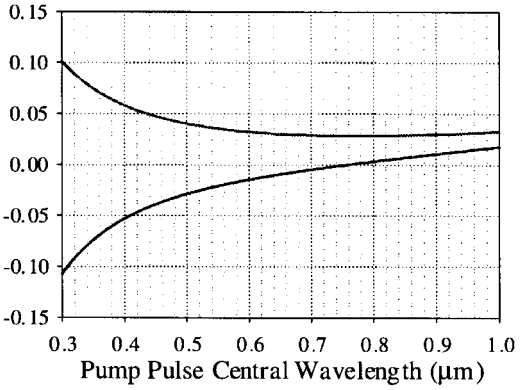

Figure 9. D_+ (lower curve) and D (upper curve), shown in units of $1/c$, for a type-II BBO crystal. Note that $D_+ = 0$ at the pump wavelength of 757 nm. The two-photon wavefunction is symmetrized at this wavelength (see figure 8).

pulsed polarization-entangled photon pairs may be generated using the well-known techniques described in [8, 10]. It is also expected that a triangularly shaped correlation function, which has been observed in CW-pumped SPDC, should be observed in ultrafast type-II SPDC, as well.

Referring to equation (5), it is clear that, if D_+/D is made to vanish, then $\Pi(t_+, t_-)$ becomes symmetric. Figure 9 shows the value of D_+ and D for a type-II BBO crystal as a function of pump pulse central wavelength. Note that $D_+ = 0$ when the central wavelength of the pump pulse is 757 nm. The two-photon wavefunction for this case is shown in figure 8 for a crystal thickness of 2 mm and a pump bandwidth of 8 nm.

In this example, this approach has an additional advantage: the entangled-photon pairs are emitted with central wavelengths of 1514 nm, which is within the standard fibre communication band. Such pulsed entangled photons at communication wavelengths may be useful for building practical quantum key distribution systems using commercially installed optical fibers. At this wavelength, of course, single photon detection is more problematic. However, the recent development of single photon counting techniques using InGa. As avalanche photodiodes may soon provide good single photon counters at this wavelength [17].

We have shown that, by making the D_+ term vanish through a careful choice of the pump wavelength, an initially asymmetric two-photon wavefunction can be made symmetric. Since the temporal and spectral properties of the photons are related by simple Fourier transforms, it should not be surprising that $D_+ = 0$ leads to a spectrally symmetric state, as well.

The spectral properties of the two-photon state from ultrafast type-II SPDC are best illustrated in plots of the two-photon joint spectrum, which can be regarded as a probability distribution for the photon frequencies. Recall that the two-photon state $|\psi\rangle$ given in equation (2) contains the phase mismatch term sincless $(\Delta L/2)$ and the pump envelope term $\mathcal{E}_p(\omega_e + \omega_o)$. The joint spectrum function is simply the square modulus of the product of these two terms:

$$S(\omega_e, \omega_o) = \left| \operatorname{sinc}\left(\frac{\Delta L}{2}\right) \mathcal{E}_p(\omega_e + \omega_o) \right|^2.$$

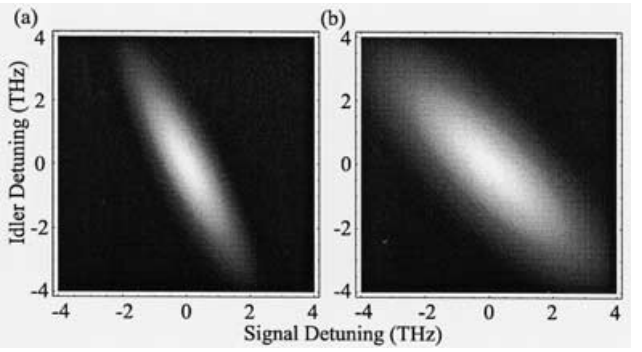

Figure 10. Calculated joint spectrum showing frequency anticorrelation between the signal and the idler photons. (*a*) Typical frequency-anticorrelated state with asymmetric joint spectrum. The pump central wavelength is 400 nm. (*b*) The asymmetry has now disappeared. The pump central wavelength is 757 nm and the bandwidth is 8 nm.

The joint spectrum function for a typical ultrafast type-II SPDC configuration (type-II BBO pumped with an ultrafast UV pulse) is shown in figure 10 (*a*). Here we have assumed that $L = 2\,\text{mm}$, the pump wavelength is 400 nm, the pump bandwidth is 2 nm and the SPDC wavelength is 800 nm. Note that the joint spectrum function is asymmetric; the frequency range of the idler photon is much larger than that of the signal. The joint spectrum becomes symmetric, however, when $D_+ = 0$, as shown in figure 10 (*b*). Note that the signal and the idler photons have identical spectra. Thus, the photon pair is distinguishable only in the polarizations of the photons, as required for a polarization-entangled state.

The spectral properties of the photon pairs represented in figure 10 (*b*) display the tendency of frequency anticorrelation in the sense that a positive detuning for one photon is accompanied by a negative detuning for the other. This effect follows from the energy conservation condition that constrains the SPDC process. In ultrafast type-II SPDC, the anticorrelation is not as strong as in the CW-pumped case owing to the broad bandwidth of the pump pulse. However, the general tendency of anticorrelation, $\omega_s = \omega_p/2 \pm \omega$ and $\omega_i = \omega_p/2 \mp \omega$ where ω is the detuning frequency, is clearly visible in figure 10. This frequency anti-correlation, however, is not a required feature of the two-photon state. In ultrafast type-II SPDC, two-photon states with novel spectral characteristics, namely the frequency-correlated state and the frequency-uncorrelated state, may be generated through appropriate choices of the parameters that affect the joint spectrum.

The idea behind two-photon states with novel spectral characteristics is not new. The output characteristics of a beam splitter and a Mach–Zehnder interferometer for frequency-correlated and frequency-uncorrelated photon pairs were theoretically studied in [18] with no discussion of how such states might be generated. Frequency-correlated states were also studied in [19], but the discussions are limited to the generation of frequency-correlated states using quasiphase matching in a periodically poled crystal. Here, we discuss how frequency-correlated states and frequency-uncorrelated states may be generated via appropriate spectral engineering of the two-photon state in ordinary bulk crystals. Since our main focus is polarization-entangled photon pairs with novel spectral

characteristics, we restrict our attention to the case in which the two-photon joint spectrum is symmetric, that is $D_+ = 0$.

Frequency-correlated state generation via the SPDC process is somewhat counter-intuitive since conservation of energy requires the frequencies of the photon pair to sum to the frequency of the pump photon. This requirement imposes a strong constraint in CW-pumped SPDC, where the pump field is monochromatic. In ultrafast SPDC, however, the pump field has a bandwidth of several terahertz in frequency (several nanometres in wavelength) and so the frequencies of the photon pair need only sum to some value within the range of pump frequencies. This extra freedom makes it possible to generate the frequency-correlated state.

Examination of the joint spectrum function $S(\omega_s, \omega_i)$ suggests that if the bandwidth of the pump envelope $\mathcal{E}_p(\omega_s + \omega_i)$ is large enough and if the parameters are chosen such that the sincless $(\Delta L/2)$ may be approximated by the delta function $\delta(\omega_s - \omega_i)$, then the two-photon state becomes

$$|\psi\rangle = C \int d\omega \, \mathcal{E}_p(2\omega) a_s^\dagger(\omega) a_i^\dagger(\omega) |0\rangle, \tag{15}$$

where C is a constant. Equation (7) shows the signature of the frequency-correlated state: $\omega_s = \omega_p/2 \pm \omega$ and $\omega_i = \omega_p/2 \pm \omega$. Figure 11 (a) shows the calculated joint spectrum function for the frequency-correlated two-photon state. In this example, the pump central wavelength was set to 757 nm in order to satisfy the condition $D_+ = 0$, that is to assure direct generation of polarization-entangled photon pairs. This also has the effect of properly aligning the sincless $(\Delta L/2)$ function. The only other requirement is that this function should be narrow enough that it may be approximated as $\delta(\omega_s - \omega_i)$. This is achieved by increasing the value of L, the crystal thickness, since the width of the sinc function is inversely proportional to the crystal length. In figure 11 (a), it is assumed that a type-II BBO crystal, 12 mm thick, is pumped by an ultrafast pulse of 20 nm bandwidth centred at 757 nm and that, at zero detuning, the wavelengths of the SPDC photons are 1514 nm. The structure of frequency correlation is clearly

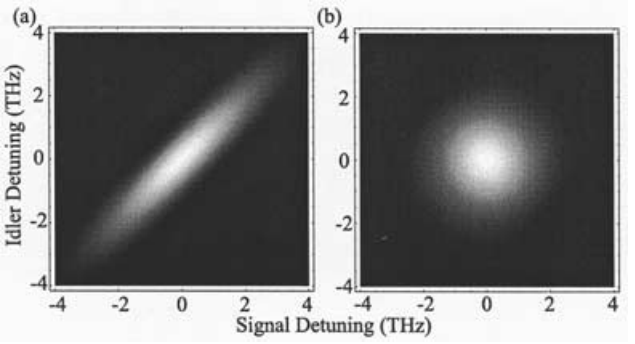

Figure 11. (a) Calculated joint spectrum showing a frequency-correlated two-photon state. The pump bandwidth is 20 nm and the crystal is type-II BBO 12 mm thick. (b) Frequency-uncorrelated state. The pump bandwidth is 10 nm and the crystal is type-II BBO 5 mm thick. The pump central wavelength is 757 nm for both cases to ensure that $D_+ = 0$ is satisfied.

illustrated: as the signal detuning increases, the idler detuning is also increased. Such frequency-correlated states have been shown to be useful for certain quantum metrology applications [5].

By slightly modifying the condition for the generation of the frequency-correlated state, it is possible to generate the frequency-uncorrelated state. By frequency-uncorrelated state, we mean that the frequencies of the two photons are uncorrelated, in the sense that the range of the available frequencies for a particular photon is completely independent of the frequency of its conjugate. As far as the photons are concerned, this means that the spectral properties of one photon are in no way correlated to the spectral properties of the other. The joint spectrum of such a state is shown in figure 11 (*b*) where the joint spectrum function is calculated for type-II SPDC in a BBO crystal 5 mm thick pumped by an ultrafast pump of 10 nm bandwidth centred at 757 nm. Again, the pump pulse central wavelength is set to 757 nm to ensure symmetry in the joint spectrum. The more general case has been discussed in [21], where it was also shown that such states are essential in experiments involving interference between photons from different SPDC sources.

5. Summary

The generation of polarization-entangled states requires the coherent superposition of two two-photon wavefunctions. An additional requirement is that the two wavefunctions must be identical in all respects except polarization. This is not the case, in general, when the photon pairs originate in a type-II SPDC process, although only a simple delay is required when the process is pumped by a CW laser. When an ultrafast pumping scheme is employed, however, these techniques typically do not result in the complete restoration of quantum interference. Some improvement is seen with thin nonlinear crystals and/or narrow spectral filters before the detectors. Unfortunately, both of these techniques result in greatly reduced count rates. By engineering the two-photon state of ultrafast type-II SPDC in time or in frequency, it is possible to recover the quantum interference without discarding any photon pairs. In addition, spectral engineering holds the promise of two-photon states with novel spectral properties that have not been available previously.

The temporal engineering of the two-photon state is accomplished through a novel interferometric technique that changes the temporal distribution of the two-photon amplitude $\mathcal{A}(t_+, t_-)$, which consists of two two-photon wavefunctions $\Pi(t_+, t_-)$. The shapes of the wavefunctions are not altered in this process, only the way in which they overlap in $\mathcal{A}(t_+, t_-)$. The temporally engineered source does not suffer the loss of quantum interference common in ultrafast type-II SPDC and the interferometer can be viewed as a universal Bell-state synthesizer since the quantum interference is independent of the crystal properties, the bandwidth of spectral filters, the bandwidth of the pump laser, and the wavelengths.

A different approach is taken in the spectral engineering technique. Here, the asymmetric two-photon wavefunction $\Pi(t_+, t_-)$ from ultrafast type-II SPDC is symmetrized through careful control of the crystal and pump properties. Such spectrally engineered two-photon states exhibit complete quantum interference with no need for auxiliary interferometric techniques. The spectral engineering techniques may also be employed in the generation of two-photon states with novel

spectral characteristics: the frequency-correlated state and the frequency uncorrelated state. Unlike typical two-photon states from the SPDC process, which exhibit strong frequency anticorrelation, the frequency-correlated state is characterized by a strong positive frequency correlation, while the frequencies of the two photons are completely uncorrelated in the frequency-uncorrelated state.

The temporal and spectral engineering techniques studied in this paper are expected to play an important role in generating the pulsed entangled photon pairs essential in applications such as practical quantum cryptography, multiphoton entangled state generation and multiphoton interference experiments. Since temporal engineering allows one to control the decoherence in a stable way, it also facilitates the study of the effects of decoherence in entangled multiqubit systems. In addition, the frequency-correlated states discussed in this paper may be useful for certain quantum metrology applications.

Acknowledgments

We would like to thank M.V. Chekhova, S.P. Kulik, M.H. Rubin and Y. Shih for helpful discussions. This research was supported in part by the US Department of Energy, Office of Basic Energy Sciences. The Oak Ridge National Laboratory is managed for the US Department of Energy by UT-Battelle, LLC, under contract DE-AC05-00OR22725.

References

[1] Einstein, A., Podolsky, B., and Rosen, N., 1935, *Phys Rev*., **47,** 777; Bell, J. S., 1987. *Speakable and Unspeakable in Quantum Mechanics* (Cambridge University Press).
[2] Stean, A., 1998, *Rep. Prog. Phys*., **61,** 117; Nielson, M. A., and Chuang, I. L., 2000, *Quantum Computation and Quantum Information* (Cambridge University Press).
[3] Boto, A. N., Kok, P., Abrams, D. S., Braunstein, S. L., Williams, C. P., and Dowling, J. P., 2000, *Phys. Rev. Lett*., **85,** 2733; D'Angelo, M., Chekhova, M. V., and Shih, Y., 2001, *Phys. Rev. Lett*., **87,** 013 602.
[4] Dowling, J. P., 1998, *Phys. Rev*. A, **57,** 4736.
[5] Jozsa, R., Abrams, D. S., Dowling, J. P., and Williams, C. P., 2000, *Phys. Rev. Lett*., **85,** 2010; Giovannetti, V., Lloyd, S., and Maccone, L., 2002, *Phys. Rev*. A, **65,** 022 309.
[6] Klyshko, D. N., 1988, *Photons and Nonlinear Optics*, New York: Gordon and Breach.
[7] Kiess, T. E., Shih, Y. H., Sergienko, A. V., and Alley, C. O., 1993, *Phys. Rev. Lett*., **71,** 3893.
[8] Shih, Y. H., and Sergienko, A. V., 1994, *Phys. Lett*. A, **186,** 29; *ibid*., **191,** 210.
[9] Rubin, M. H., Klyshko, D. N., Shih, Y. H., and Sergienko, A. V., 1994, *Phys. Rev*. A, **50,** 5122.
[10] Kwiat, P. G., Mattle, K., Weinfurter, H., Zeilinger, A., Sergienko, A. V., and Shih, Y., 1995, *Phys. Rev. Lett*., **75,** 4337.
[11] Keller, T. E., Rubin, M. H., Shih, Y., and Wu, L.-A., 1998, *Phys. Rev*. A, **57,** 2076.
[12] De Caro, L., and Garuccio, A., 1994, *Phys. Rev*. A, **50,** R2803; Popescu, S., Hardy, L., and Zukowski, M., 1997, *Phys. Rev*. A, **56,** R4353 (1997); Zukowski, M., Kaszlikowski, D., and Santos, E., 1999, *Phys. Rev*. A, **60,** R2614.
[13] Keller, T. E., and Rubin, M. H., 1997, *Phys. Rev*. A, **56,** 1534 (1997); Grice, W. P., and Walmsley, I. A., 1997, *Phys. Rev*. A, **56,** 1627.
[14] Di Guiseppe, G., Haiberger, L., De Martini, F., and Sergienko, A. V., 1997, *Phys. Rev*. A, **56,** R21; Grice, W. P., Erdmann, R., Walmsley, I. A., and Branning, D., 1998, *Phys. Rev*. A, **57,** R2289; Kim, Y.-H., Berardi, V., Chekhova, M. V., and

Shih, Y., 2001, *Phys. Rev.* A, **64,** 011 801(R); Kim, Y.-H., Kulik, S. P., Rubin, M. H., and Shih, Y., 2001, *Phys. Rev. Lett.*, **86,** 4710.

[15] Branning, D., Grice, W. P., Erdmann, R., and Walmsley, I. A., 1999, *Phys. Rev. Lett.*, **83,** 955; Shaprio, J. H, and Wang, F. N. C., 2000, *J. Optics* B, **2,** L1; Kim, Y.-H., Chekhova, M. V., Kulik, S. P., Rubin, M. H., and Shih, Y., 2001, *Phys. Rev.* A, **63,** 062 301; Burlakov, A. V., Chekhova, M. V., Karabutova, O. A., and Kulik, S. P., 2001, *Phys. Rev.* A, **64,** 041 803(R).

[16] Werner, R. F., 1989, *Phys. Rev.* A, **40,** 4277; Kwiat, P. G., Barraza-Lopez, S., Stefanov, A., and Gisin, N., 2001, *Nature*, **409,** 1014; White, A. G., James, D. F. V., Munro, W. J., and Kwiat, P. G., 2001, *Phys. Rev.* A, **65,** 012 301.

[17] Lacaita, A., Zappa, F., Cova, S., and Lovati, P., 1996, *Appl. Optics–OT*, **35,** 2986; Ribordy, G., Gautier, J.-D., Zbinden, H., and Gisin, N., 1998, *Appl. Optics–LT*, **37,** 2272; Karlsson, A., Bourennane, M., Ribordy, G., Zbinden, H., Brendel, J., Rarity, J., and Tapster, P., 1999, *IEEE Circuits and Devices*, November 34; Hiskett, P. A., Buller, G. S., Loudon, A. Y., Smith, J. M., Gontijo, I., Walker, A. C., Townsend, P. D., and Robertson, M. J., 2000, *Appl. Optics–LT*, **39,** 6818.

[18] Campos, R. A., Saleh, B. E. A., and Teich, M. C., 1990, *Phys. Rev.* A, **42,** 4127.

[19] Giovannetti, V., Maccone, L., Shapiro, J. H., and Wong, F. N. C., 2001 quant-ph/0109135.

[20] Grice, W. P., U'Ren, A. B., and Walmsley, I. A., 2001, *Phys. Rev.* A, **64,** 063 815.